SUPPLEMENTAL DATASETS, TABLES AND FIGURES

Dataset S1. list of the Mlh3 ChIP-seq peaks (Excel spreadsheet)

Dataset S2. list of the *pCUP1-IME1* synchronized Spo11 oligonucleotides hotspots (Excel spreadsheet)

Dataset S3. Mlh3-Flagged pulled-down proteins (Excel spreadsheet)

Dataset S4. Primary data underlying all graphs (Excel spreadsheet)

Table S1. Strains used in this study

Table S2. Strains used in the different figures

Table S1: Genotypes of strains used in this study.

Diploids : The MATa parent is indicated first

Strain name	Genotype
VBD1311	*a/l ho::hisG/" leu2::hisG/'' ura3/'' HIS4::LEU2-(BamH1; +ori)/his4-X::LEU2-(NgoMIV; +ori)-URA3*
VBD1674	*a/l ho::hisG/" leu2::hisG/'' ura3/'' HIS4::LEU2-(BamH1; +ori)/his4-X::LEU2- (NgoMIV; +ori)-URA3 MLH3-512-His6-Flag3-515::HphMX/"*
VBD1861	*a/l ho::hisG/" leu2::hisG/'' ura3/'' HIS4::LEU2-(BamH1; +ori)/his4-X::LEU2-(BamH1; +ori)-URA3 MLH3-512-Myc18-515::HphMX/"*
VBD1599	*a/l ho::hisG/" leu2::hisG/'' ura3/'' HIS4::LEU2-(BamH1; +ori)/his4-X::LEU2-(NgoMIV; +ori)-URA3 MLH3-512-Myc8-515::HphMX/"*
VBD1749	*a/l ho::hisG/" leu2::hisG/'' ura3/'' HIS4::LEU2-(BamH1; +ori)/his4-X::LEU2-(BamH1; +ori)-URA3 mlh3Δ::HphMX/"*
FK3088	*a/l ho::LYS2/" ura3/'' his3::hisG/'' leu2::hisG/" trp1::hisG/''*
FK7795	*a/l ho::LYS2/" ura3/'' his3::hisG/'' leu2::hisG/" trp1::hisG/'' MLH3-512-Myc18-515::KanMX MSH4-HA3::KanMX*
FK8312	*a/l ho::LYS2/" ura3/'' his3::hisG/'' leu2::hisG/" trp1::hisG/'' MLH3-512-Myc18-515::KanMX zip3Δ::KanMX*
VBD2096	*a/l ho::hisG/" leu2::hisG/'' ura3/'' HIS4::LEU2-(BamH1; +ori)/his4-X::LEU2-(BamH1; +ori)-URA3 MLH3-512-Myc18-515::HphMX/" msh4Δ::NatMX/"*
VBD1864	*a/l ho::hisG/" leu2::hisG/'' ura3/'' HIS4::LEU2-(BamH1; +ori)/his4-X::LEU2-(BamH1; +ori)-URA3 MLH3-512-Myc18-515::HphMX/" ndt80Δ::NatMX/"*
VBD1716	*a/l ho::hisG/" leu2::hisG/'' ura3/'' HIS4::LEU2-(BamH1; +ori)/his4-X::LEU2-(BamH1; +ori)-URA3 MLH3-512-Myc8-515::HphMX/"*
VBD1616	*a/l ho::hisG/" leu2::hisG/'' ura3/'' HIS4::LEU2-(BamH1; +ori)/his4-X::LEU2-(NgoMIV; +ori)-URA3 MLH3-512-Myc8-515::HphMX/" spo11Δ::HphMX/"*
VBD1928	*a/l ho::hisG/" leu2::hisG/'' ura3/'' HIS4::LEU2-(BamH1; +ori)/his4-X::LEU2-(BamH1; +ori)-URA3 MLH3-512-Myc8-515::HphMX/" mer3Δ:: HphMX/"*
VBD1729	*a/l ho::hisG/" leu2::hisG/'' ura3/'' HIS4::LEU2-(BamH1; +ori)/his4-X::LEU2-(BamH1; +ori)-URA3 MLH3-512-Myc8-515::HphMX/" msh4Δ::HphMX/"*
VBD1734	*a/l ho::hisG/" leu2::hisG/'' ura3/'' HIS4::LEU2-(BamH1; +ori)/his4-X::LEU2-(BamH1; +ori)-URA3 MLH3-512-Myc8-515::HphMX/" exo1Δ::NatMX/"*
VBD1728	*a/l ho::hisG/" leu2::hisG/'' ura3/'' HIS4::LEU2-(BamH1; +ori)/his4-X::LEU2-(BamH1; +ori)-URA3 MLH3-512-Myc8-515-D523N::HphMX/"*
VBD1730	*a/l ho::hisG/" leu2::hisG/'' ura3/'' HIS4::LEU2-(BamH1; +ori)/his4-X::LEU2-(BamH1; +ori)-URA3 MLH3-512-Myc8-515::HphMX/" ndt80Δ::NatMX/"*
VBD1834	*a/l ho::hisG/" leu2::hisG/'' ura3/ura3::BrdUInc-URA3 HIS4::LEU2-(BamH1; +ori)/his4-X::LEU2-(NgoMIV; +ori)-URA3 irt1::KanMX-pCUP1-3HA-IME1/''*
VBD1421	*a/l ho::hisG/" leu2::hisG/'' ura3/'' HIS4::LEU2-(BamH1; +ori)/his4-X::LEU2-(NgoMIV; +ori)-URA3 MER3-linker-His6Flag3::NatMX/"*
VBD1841	*a/l ho::hisG/" leu2::hisG/'' ura3/'' HIS4::LEU2-(BamH1; +ori)/his4-X::LEU2-(BamH1; +ori)-URA3 MLH3-512-Myc8-515::HphMX/" spo11Δ::HphMX/" irt1::KanMX-pCUP1-3HA-IME1/''*

VBD2026 *a/l ho::hisG/" leu2::hisG/'' ura3/'' HIS4::LEU2-(BamH1; +ori)/his4-X::LEU2-(BamH1; +ori)-URA3 MLH3-512-Myc8-515::HphMX/" exo1D173A/" irt1::KanMX-pCUP1-3HA-IME1/''*

VBD2016 *a/l ho::hisG/" leu2::hisG/'' ura3/'' HIS4::LEU2-(BamH1; +ori)/his4-X::LEU2-(BamH1; +ori)-URA3 Spo11-His6-Flag3::NatMX/" irt1::KanMX-pCUP1-3HA-IME1/''*

VBD1810 *a/l ho::hisG/" leu2::hisG/'' ura3/'' HIS4::LEU2-(BamH1; +ori)/his4-X::LEU2-(BamH1; +ori)-URA3 MLH3-512Myc8-515::HphMX/" MLH1-710-HA6-713::KanMX/''*

VBD1812 *a/l ho::hisG/" leu2::hisG/'' ura3/'' HIS4::LEU2-(BamH1; +ori)/his4-X::LEU2-(BamH1; +ori)-URA3 MLH1-710-HA6-713::KanMX/'' PMS1-758-His6-Flag3-761::NatMX/"*

VBD1811 *a/l ho::hisG/" leu2::hisG/'' ura3/'' HIS4::LEU2-(BamH1; +ori)/his4-X::LEU2-(BamH1; +ori)-URA3 MLH3-512Myc8-515::HphMX/" MLH1-710-HA6-713::KanMX/'' PMS1-758-His6-Flag3-761::NatMX/"*

VBD1906 *a/l ho::hisG/" leu2::hisG/'' ura3/'' HIS4::LEU2-(BamH1; +ori)/his4-X::LEU2-(NgoMIV; +ori)-URA3 MLH3-512Myc8-515::HphMX/MLH3-512-His6-Flag3-515::HphMX*

VBD1993 *a/l ho::hisG/" leu2::hisG/'' ura3/'' HIS4::LEU2-(BamH1; +ori)/his4-X::LEU2-(NgoMIV; +ori)-URA3 MLH3-512-His6-Flag3-515::HphMX/" MLH1-710-HA6-713::KanMX/''*

VBD1991 *a/l ho::hisG/" leu2::hisG/'' ura3/'' his4-X::LEU2-(BamH1; +ori)-URA3/HIS4::LEU2-(BamH1; +ori) MLH3-512-His6-Flag3-515::HphMX/" MLH1-710-HA6-713::KanMX/'' EXO1-TAP::URA3/"*

VBD1996 *a/l ho::hisG/" leu2::hisG/'' ura3/'' HIS4::LEU2-(BamH1; +ori)/his4-X::LEU2-(BamH1; +ori)-URA3 MLH3-512-His6-Flag3-515::HphMX/" mlh1- E682A-710-HA6-713::KanMX/'' EXO1-TAP::URA3/"*

VBD1992 *a/l ho::hisG/" leu2::hisG/'' ura3/'' HIS4::LEU2-(BamH1; +ori)/his4-X::LEU2-(BamH1; +ori)-URA3 MLH3-512-His6-Flag3-515::HphMX/" MLH1-710-HA6-713::KanMX/'' MSH4-TAP::URA3/"*

VBD2072 *a/l ho::hisG/" leu2::hisG/'' ura3/" HIS4::LEU2-(BamH1; +ori)/his4-X::LEU2-(BamH1; +ori)-URA3 irt1::KanMX-pCUP1-3HA-IME1/'' MLH1-710-6HA-713::NatMX/" MLH3-512-8Myc-515::HphMX/"*

VBD2071 *a/l ho::hisG/" leu2::hisG/'' ura3/" HIS4::LEU2-(BamH1; +ori)/his4-X::LEU2-(BamH1; +ori)-URA3 irt1::KanMX-pCUP1-3HA-IME1/'' MLH1-710-6HA-713::NatMX/" MLH3-512-8Myc-515::HphMX/" CDC5-TAP::URA3/"*

VBD2090 *a/l ho::hisG/" leu2::hisG/'' ura3/" HIS4::LEU2-(BamH1; +ori)/his4-X::LEU2-(BamH1; +ori)-URA3 irt1::KanMX-pCUP1-3HA-IME1/'' EXO1-Myc13::HphMX/"*

VBD2081 *a/l ho::hisG/" leu2::hisG/'' ura3/" HIS4::LEU2-(BamH1; +ori)/his4-X::LEU2-(BamH1; +ori)-URA3 irt1::KanMX-pCUP1-3HA-IME1/'' EXO1-Myc13::HphMX/" CDC5-TAP::URA3/"*

VBD1837 *a/l ho::hisG/" leu2::hisG/'' ura3/'' HIS4::LEU2-(BamH1; +ori)/his4-X::LEU2-(BamH1; +ori)-URA3 MLH3-512-Myc8-515::HphMX/" irt1::KanMX-pCUP1-3HA-IME1/''*

VBD2095 *a/l ho::hisG/" leu2::hisG/'' ura3/" HIS4::LEU2-(BamH1; +ori)/his4-X::LEU2-(BamH1; +ori)-URA3 irt1::KanMX-pCUP1-3HA-IME1/'' MLH1-710-6HA-713::NatMX/" MLH3-512-8Myc-515::HphMX/" CDC5-TAP-URA3/" exo1Δ::NatMX/"*

VBD2113 *a/l ho::hisG/" leu2::hisG/'' ura3/" HIS4::LEU2-(BamH1; +ori)/HIS4::LEU2-(BamH1; +ori) irt1::KanMX-pCUP1-3HA-IME1/'' MLH1-710-6HA-713::NatMX/" EXO1-Myc13::HphMX/"*

VBD2111 *a/l ho::hisG/" leu2::hisG/'' ura3/" HIS4::LEU2-(BamH1; +ori)/HIS4::LEU2-(BamH1; +ori) irt1::KanMX-pCUP1-3HA-IME1/'' MLH1-710-6HA-713::NatMX/" EXO1-Myc13::HphMX/" CDC5-TAP::URA3/"*

VBD2112 *a/l ho::hisG/" leu2::hisG/'' ura3/" HIS4::LEU2-(BamH1; +ori)/HIS4::LEU2-(BamH1; +ori) irt1::KanMX-pCUP1-3HA-IME1/'' mlh1E682A-710-6HA-713::NatMX/" EXO1-Myc13::HphMX/" CDC5-TAP-URA3/"*

VBD2167 *a/l ho::hisG/" leu2::hisG/'' ura3/" HIS4::LEU2-(BamH1; +ori)/his4-X::LEU2-(BamH1; +ori)-URA3 irt1::KanMX-pCUP1-3HA-IME1/'' MLH1-710-6HA-713::NatMX/" exo1-cid-Myc13::HphMX/" CDC5-TAP::URA3/"*

VBD2159 *a/l ho::hisG/" leu2::hisG/'' ura3/" HIS4::LEU2-(BamH1; +ori)/his4-X::LEU2-(BamH1; +ori)-URA3 EXO1-Myc13::HphMX/"*

VBD2161 *a/l ho::hisG/" leu2::hisG/'' ura3/" HIS4::LEU2-(BamH1; +ori)/his4-X::LEU2-(BamH1; +ori)-URA3 exo1-cid-Myc13::HphMX/"*

VBD2160 *a/l ho::hisG/" leu2::hisG/'' ura3/" HIS4::LEU2-(BamH1; +ori)/his4-X::LEU2-(BamH1; +ori)-URA3 exo1Δ::NatMX/"*

VBD2162 *a/l ho::hisG/" leu2::hisG/'' ura3/" HIS4::LEU2-(BamH1; +ori)/his4-X::LEU2-(BamH1; +ori)-URA3 pCLB2-3HA-MMS4::kanMX4/" slx4Δ::HphMX/" yen1Δ::HphMX/" EXO1-Myc13::HphMX/"*

VBD2163 *a/l ho::hisG/" leu2::hisG/'' ura3/" HIS4::LEU2-(BamH1; +ori)/his4-X::LEU2-(BamH1; +ori)-URA3 pCLB2-3HA-MMS4::kanMX4/" slx4Δ::HphMX/" yen1Δ::HphMX/" exo1-cid-Myc13::HphMX/"*

VBD2164 *a/l ho::hisG/" leu2::hisG/'' ura3/" his4-X::LEU2-(BamH1; +ori)-URA3/ HIS4::LEU2-(BamH1; +ori) pCLB2-3HA-MMS4::kanMX4/" slx4Δ::HphMX/" yen1Δ::HphMX/" exo1Δ::NatMX/"*

VBD2169 *a/l ho::LYS2 leu2::hisG/'' trp1::hisG/" ura3/'' CEN8/CEN8::tdTomato-LEU2 ARG4/ARG4::GFP*-URA3 THR1::m-Cerulean-TRP1/THR1 EXO1-Myc13::HphMX/"*

VBD2170 *a/l ho::LYS2 leu2::hisG/'' trp1::hisG/" ura3/'' CEN8/CEN8::tdTomato-LEU2 ARG4/ARG4::GFP*-URA3 THR1::m-Cerulean-TRP1/THR1 exo1-cid-Myc13::HphMX/"*

VBD2172 *a/l ho::LYS2 leu2::hisG/'' trp1::hisG/" ura3/'' CEN8/CEN8::tdTomato-LEU2 ARG4/ARG4::GFP*-URA3 THR1::m-Cerulean-TRP1/THR1 exo1Δ::HphMX/"*

VBD2176 *a/l ho::LYS2 leu2::hisG/'' trp1::hisG/" ura3/'' CEN8/CEN8::tdTomato-LEU2 ARG4/ARG4::GFP*-URA3 THR1::m-Cerulean-TRP1/THR1 pCLB2-3HA-MMS4::kanMX4/" EXO1-Myc13::HphMX/"*

VBD2178 *a/l ho::LYS2 leu2::hisG/'' trp1::hisG/" ura3/'' CEN8/CEN8::tdTomato-LEU2 ARG4/ARG4::GFP*-URA3 THR1::m-Cerulean-TRP1/THR1 pCLB2-3HA-MMS4::kanMX4/" exo1-cid-Myc13::HphMX/"*

VBD2180 *a/l ho::LYS2 leu2::hisG/'' trp1::hisG/" ura3/'' CEN8/CEN8::tdTomato-LEU2 ARG4/ARG4::GFP*-URA3 THR1::m-Cerulean-TRP1/THR1 pCLB2-3HA-MMS4::kanMX4/" exo1Δ::HphMX/"*

VBD2224 *a/l ho::hisG/" leu2::hisG/'' ura3/" HIS4::LEU2-(BamH1; +ori)/his4-X::LEU2-(BamH1; +ori)-URA3 pCLB2-3HA-MMS4::kanMX4/" slx4Δ::HphMX/" yen1Δ::HphMX/" exo1-cid-Myc13::HphMX/exo1-cid-CDC5-TAP::URA3*
VBD2220 *a/l ho::hisG/" leu2::hisG/'' ura3/" HIS4::LEU2-(BamH1; +ori)/his4-X::LEU2-(BamH1; +ori)-URA3 pCLB2-3HA-MMS4::kanMX4/" slx4Δ::HphMX/" yen1Δ::HphMX/" exo1-cid-Myc13::HphMX/" exo1-cid-Cdc5-N209A-TAP::URA3*
VBD2222 *a/l ho::hisG/" leu2::hisG/'' ura3/" HIS4::LEU2-(BamH1; +ori)/his4-X::LEU2-(BamH1; +ori)-URA3 pCLB2-3HA-MMS4::kanMX4/" slx4Δ::HphMX/" yen1Δ::HphMX/" exo1-cid-Myc13::HphMX/"pEXO1-CDC5-TAP::URA3*
VBD2070 *a/l ura3/" lys2/" ho::LYS2/" arg4Δ(eco47III-hpa1)/" cyh2-z ndt80Δ(Eco47III-BseRI)::kanMX6/" EXO1-TAP::URA3/" pCDC5-CDC5-pFA6a-pGPD1-GAL4(1-848)-ER-NatMX4-pGAL1-CDC5/"*
VBD2134 *a/l ho::hisG/" leu2::hisG/'' ura3/" HIS4::LEU2-(BamH1; +ori)/his4-X::LEU2-(BamH1; +ori) irt1::KanMX-pCUP1-3HA-IME1/'' EXO1-Myc13::HphMX/"*
VBD2131 *a/l ho::hisG/" leu2::hisG/'' ura3/" HIS4::LEU2-(BamH1; +ori)/his4-X::LEU2-(BamH1; +ori) irt1::KanMX-pCUP1-3HA-IME1/'' exo1-S663AS664A-Myc13::HphMX/"*
VBD2141 *a/l ho::hisG/" leu2::hisG/'' ura3/" HIS4::LEU2-(BamH1; +ori)/his4-X::LEU2-(BamH1; +ori)-URA3 irt1::KanMX-pCUP1-3HA-IME1/'' exo1-9A-Myc13::HphMX/"*
VBD2133 *a/l ho::hisG/" leu2::hisG/'' ura3/" HIS4::LEU2-(BamH1; +ori)/his4-X::LEU2-(BamH1; +ori) irt1::KanMX-pCUP1-3HA-IME1/'' exo1Δ::HphMX/"*

Haploids

Strain name	**Genotype**
VBH854	*MATl ade5-1 lys2::InsE-A14 trp1-289 his7-2 leu2-3,112 ura3-52*
VBH1874	*MATl ade5-1 lys2::InsE-A14 trp1-289 his7-2 leu2-3,112 ura3-52 mlh3Δ::HphMX*
VBH2513	*MATl ade5-1 lys2::InsE-A14 trp1-289 his7-2 leu2-3,112 ura3-52 MLH3-512-His6-Flag3-515::HphMX*
VBH2510	*MATl ade5-1 lys2::InsE-A14 trp1-289 his7-2 leu2-3,112 ura3-52 MLH3-512Myc18-515::HphMX*
VBH2507	*MATl ade5-1 lys2::InsE-A14 trp1-289 his7-2 leu2-3,112 ura3-52 MLH3-512Myc8-515::HphMX*

Table S2: Strains used in the different figures.

Fig. 1B: FK3088; VBD1861.
Fig. 1C: FK7795.
Fig. 1F: FK8312.
Fig. 1G: VBD2096.
Fig. 1J: VBD1864.
Fig. 2A: VBD1716**;** VBD1616**;** VBD1728**;** VBD1928**;** VBD1729**;** VBD1734**;** VBD1730.
Figs. 2B and C: VBD1421; VBD1837; VBD1841.
Figs. 2D and F: VBD1421; VBD1837; VBD1841; VBD2016.
Fig. 2E: VBD1837; VBD1841; VBD2016.
Fig. 3A: VBD1311; VBD1674.
Fig. 3B: VBD1311; VBD1993; VBD1991; VBD1996; VBD1992.
Fig. 3C: VBD1311; VBD1991.
Fig. 3D: VBD1810; VBD1812; VBD1811; VBD1716; VBD1906
Fig. 4A: VBD1834; VBD2072; VBD2071; VBD2090; VBD2081.
Fig. 4B: VBD1837; VBD2071.
Fig. 4C: VBD1834; VBD2072; VBD2071; VBD2095.
Fig. 4D: VBD1834; VBD2113; VBD2111; VBD2112.
Fig. 6A: VBD2113; VBD2111; VBD2167.
Fig. 6B: VBD2159; VBD2161; VBD2160; VBD2162; VBD2163; VBD2164.
Fig. 6C: VBD2169; VBD2170; VBD2172; VBD2176; VBD2178; VBD2180.
Fig. 6D: VBD2163; VBD2224; VBD2220; VBD2222.
SI Appendix, Figs. S1A and B: VBD1311; VBD1674; VBD1861; VBD1599; VBD1749.
SI Appendix, Fig. S1C: VBH854; VBH2513; VBH2510; VBH2507; VBH1874.
SI Appendix, Fig. S2: VBD1716**;** VBD1616**;** VBD1728**;** VBD1928**;** VBD1729**;** VBD1734**;** VBD1730.
SI Appendix, Fig. S3: VBD1834.
SI Appendix, Figs. S4C and D: VBD1837; VBD2026; VBD1841.
SI Appendix, Fig. S6: VBD1716; VBD1906; VBD1811.
SI Appendix, Fig. S8A: VBD2070
SI Appendix, Fig. S8C: VBD2134; VBD2131; VBD2141; VBD2133.

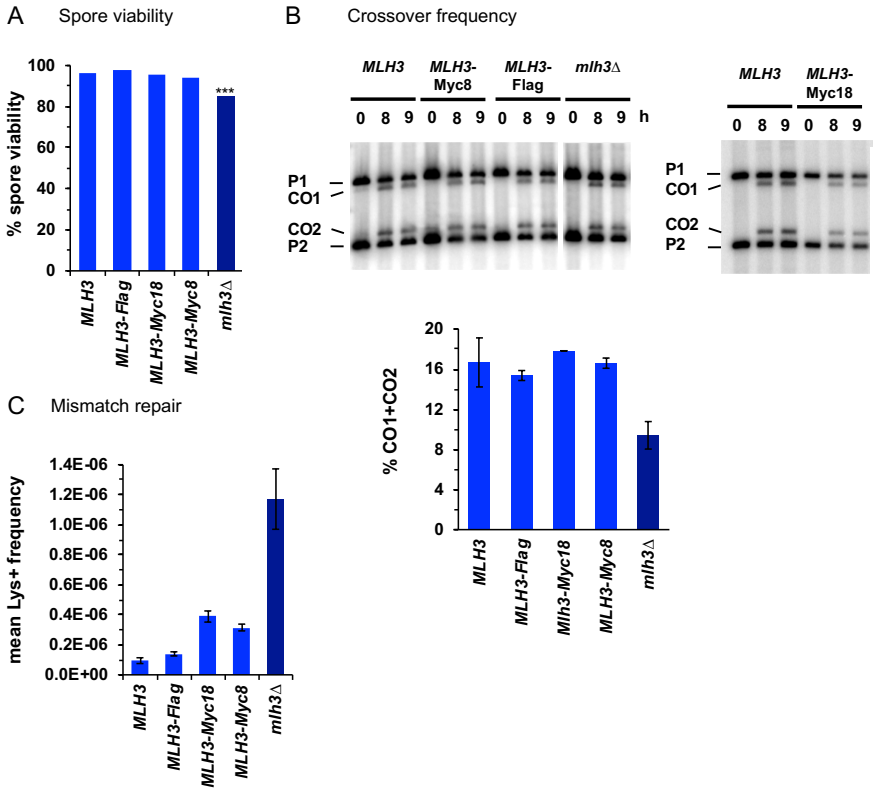

Figure S1. Mlh3 alleles tagged internally in the C terminal domain are functional for meiotic recombination and mismatch repair

(A) Spore viability of diploid SK1 strains bearing the indicated *MLH3* genotype at its endogenous locus. *MLH3* (188 tetrads), *MLH3*-Flag (114 tetrads), *MLH3*-Myc18 (104 tetrads), *MLH3*-Myc8 (117 tetrads), *mlh3Δ* (109 tetrads). ***$p<4.10^{-11}$, Fisher's exact test between *MLH3* and *mlh3Δ*.

(B) Crossover frequency at the *HIS4LEU2* hotspot monitored by Southern blot at the indicated times in meiosis. Positions of parental bands (P1 and P2) and of the recombinant crossover products (CO1 and CO2) are indicated. Graphs show quantification at 9 h from two (three for *MLH3*) independent biological replicates ± S.D.. Same strains as in (A).

(C) Mutator assay. Frequency of reversion to Lys+ in haploid vegetative cells containing the indicated *MLH3* genotype at its endogenous locus. Values are the mean ± S.E.M. of 9 independent colonies.

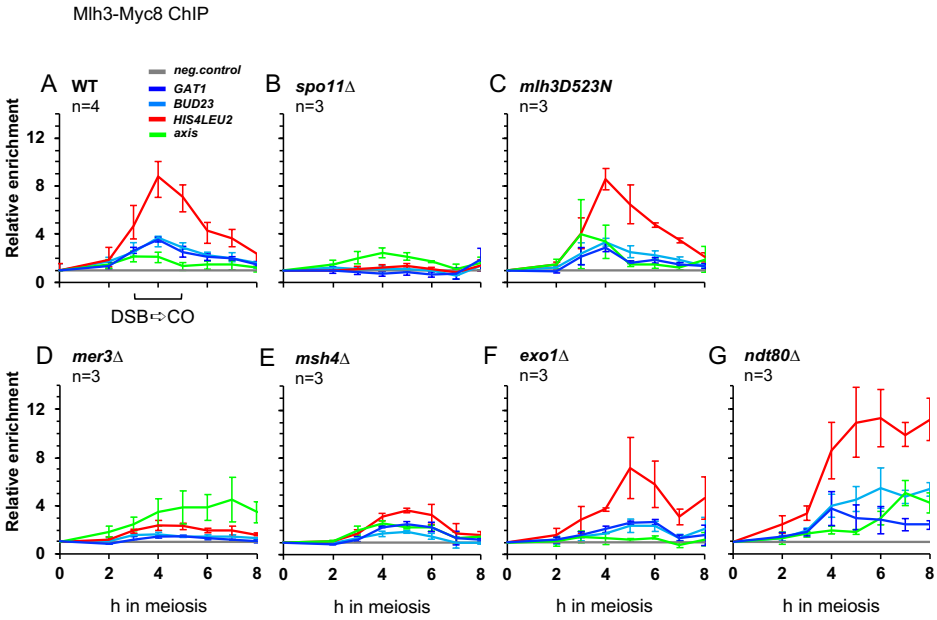

Figure S2: Mlh3 associates with meiotic DSB hotspots at a late step of recombination, independently of *NDT80* activation

(A) to (G) Mlh3-Myc levels at the three indicated meiotic DSB hotspots and one axis-associated site relative to a negative control site (*NFT1)* assessed by ChIP and qPCR during meiotic time-courses. Values are the mean ± S.E.M. from three (four in WT) independent experiments.

(A) WT, (B) *spo11Δ*, (C) *mlh3D523N*, (D) *mer3Δ*, (E) *msh4Δ*, (F) *exo1Δ*, (G) *ndt80Δ*.

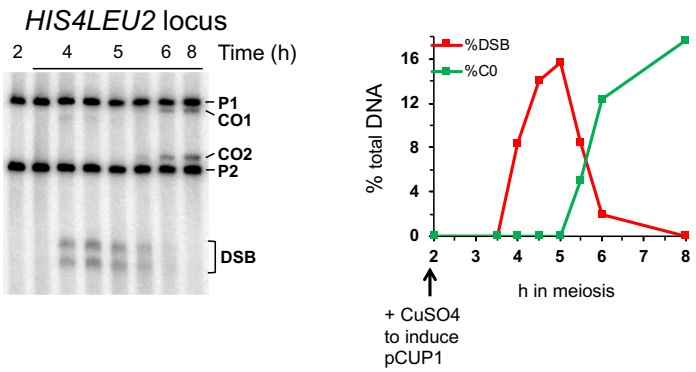

Figure S3: Timing of DSB and crossover formation in p*CUP1-IME1* synchronized meiosis

Cu^{++} is added at the 2 h time-point to induce *IME1* expression. DSB and crossover formation is followed at the *HIS4LEU2* hotspot by Southern blot analysis. Positions of parental bands (P1 and P2) and of the recombinant crossover products (CO1 and CO2) are indicated. The graph shows quantification of DSB and crossover frequencies.

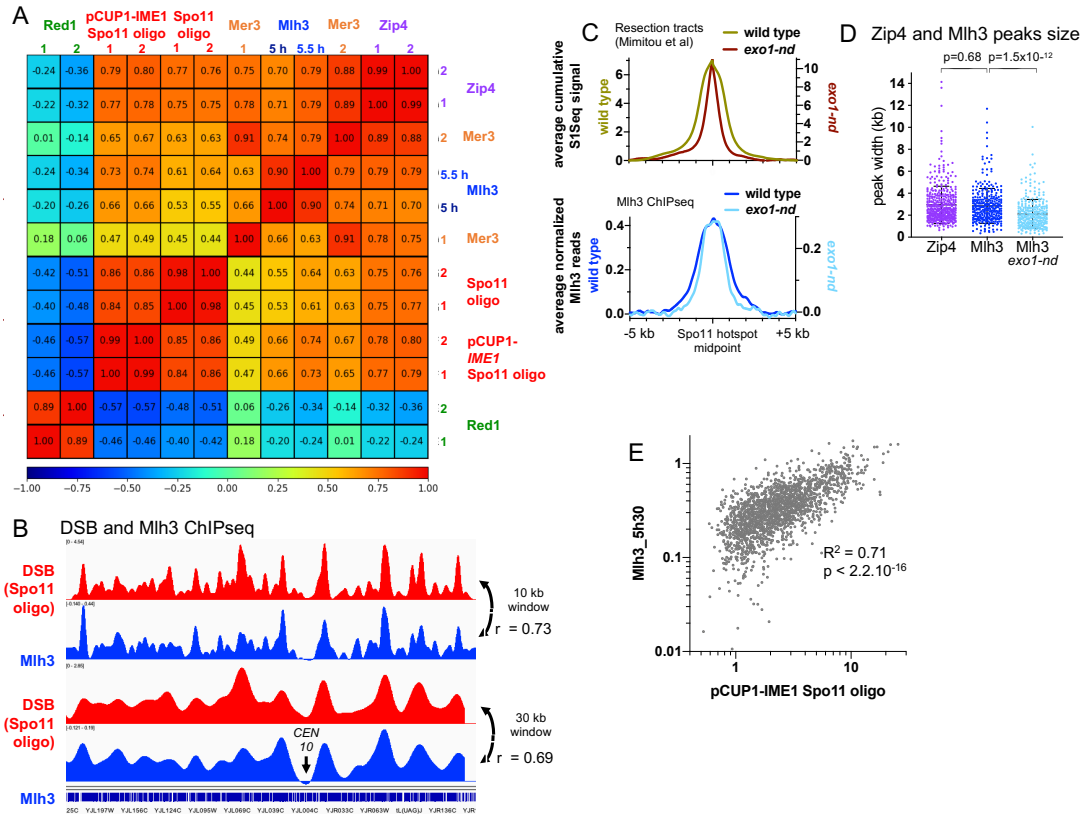

Figure S4: Correlation between Mlh3 binding sites and DSBs, ZMM and axis protein binding sites

(A) Correlation heatmap between the indicated binding profiles. For each replicate, normalized binding data of the indicated protein were used after smoothing with a 2000 bp window. Zip4 data are from (1), Spo11 oligo data are from (2) and Red1 data are from (3). The comparison was made on the regions encompassing the Red1 peaks (933 peaks) (3), the top 1000 Spo11 oligo hotspots (2) and the top 1000 Mlh3 peaks determined at 5.5 h (see Dataset S1). The Spearman correlation coefficient is indicated for each pair-wise comparison.

(B) Chromosome-wide correlation between DSB (p*CUP1-IME1* Spo11 oligos) and Mlh3, at two different smoothing scales. The correlation coefficient (Spearman) along the whole genome is indicated for each comparison.

(C) Average ChIP-seq signal of Mlh3 (5.5 h timepoint) compared to the distribution of resection tracts computed from resection endpoints (data from (4), see Methods). Resection tracts are measured at the 500 strongest Spo11 hotspots from (2), whereas Mlh3 ChIP-seq signal (smoothed with a 200 bp window) is aligned on the 500 strongest p*CUP1-IME1* Spo11 hotspots (this study).

(D) Width of Zip4 and Mlh3 peaks at the DSB hotspots. Only peaks that match with at least one of the strongest 500 Spo11 hotspots are considered (for Zip4, 421 peaks (Spo11 hotspots from (2); for Mlh3 and Mlh3 *exo1-nd*, 318 and 300 peaks, respectively (p*CUP1-IME1* Spo11 spots)). A Mann-Whitney-Wilcoxon test was used to compare the datasets.

(E) Correlation between Mlh3 and DSB frequency at the Spo11 hotspots. The signal intensities at the locations comprised in the strongest Spo11 hotspots+1kb on each side were computed for each interstitial hotspot (further than 40 kb or 20 kb from a telomere or centromere, respectively). The Pearson correlation coefficient is indicated as well as the associated pvalue.

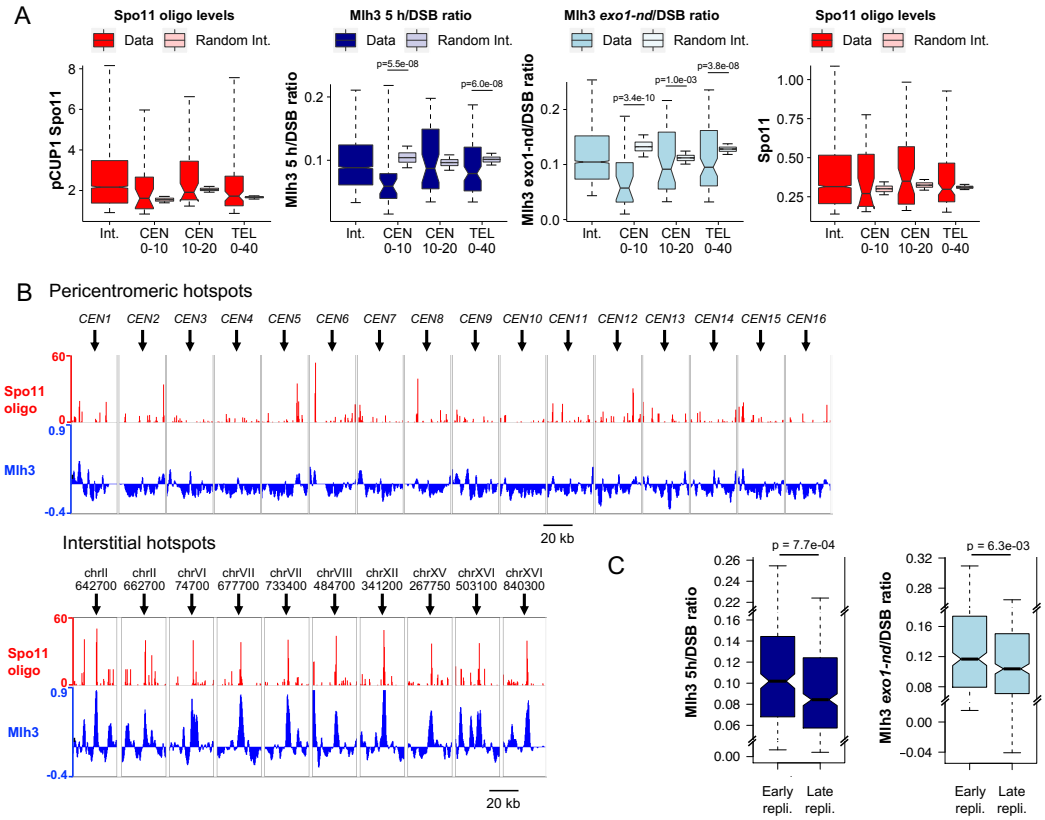

Figure S5: Mlh3 signals per DSB in proximity to a centromere or a telomere and in early versus late replicated regions

(A) The Spo11 oligo levels or the ratio of Mlh3 ChIP-seq signal over the corresponding pCUP1-IME1 Spo11 oligo signal was computed on the width plus 1 kb on each side of the strongest corresponding 2000 Spo11 hotspots at the indicated chromosome regions: interstitial (1829 hotspots); 0 to10 kb from a centromere (28 hotspots); 10 to 20 kb from a centromere (46 hotspots); 0 to 40 kb from a telomere (97 hotspots). For each region, the corresponding interstitial control was computed by randomly selecting groups of interstitial hostpots regions with the same median Spo11 oligo level, this step was repeated 10000 times. Statistical differences (Mann-Whitney-Wilcoxon test) between different regions and their interstitial control are indicated.

(B) DSB (p*CUP1-IME1* Spo11 oligo) and Mlh3 binding at the 16 centromeres (top panels) and in 10 interstitial regions with similar DSB frequency (lower panels). The normalized signal smoothed with a 200 bp window size is indicated.

(C) Early and late replicating regions as in Figure 2F. Data are represented as boxplots, and the statistical differences (Mann-Whitney-Wilcoxon test) between different regions are indicated.

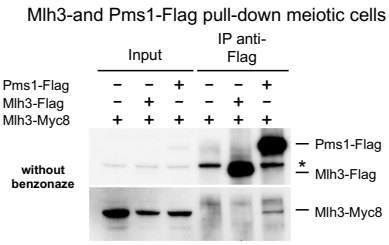

Figure S6: Mlh3 interacts with Pms1 but not with Mlh3 in meiotic cells
Coimmunoprecipitation between Pms1 and Mlh3 or Mlh3 and itself in meiotic cells at 4 h in meiosis, in the absence of benzonase treatment and analyzed by Western blot (same as Figure 3D except that benzonase was omitted).

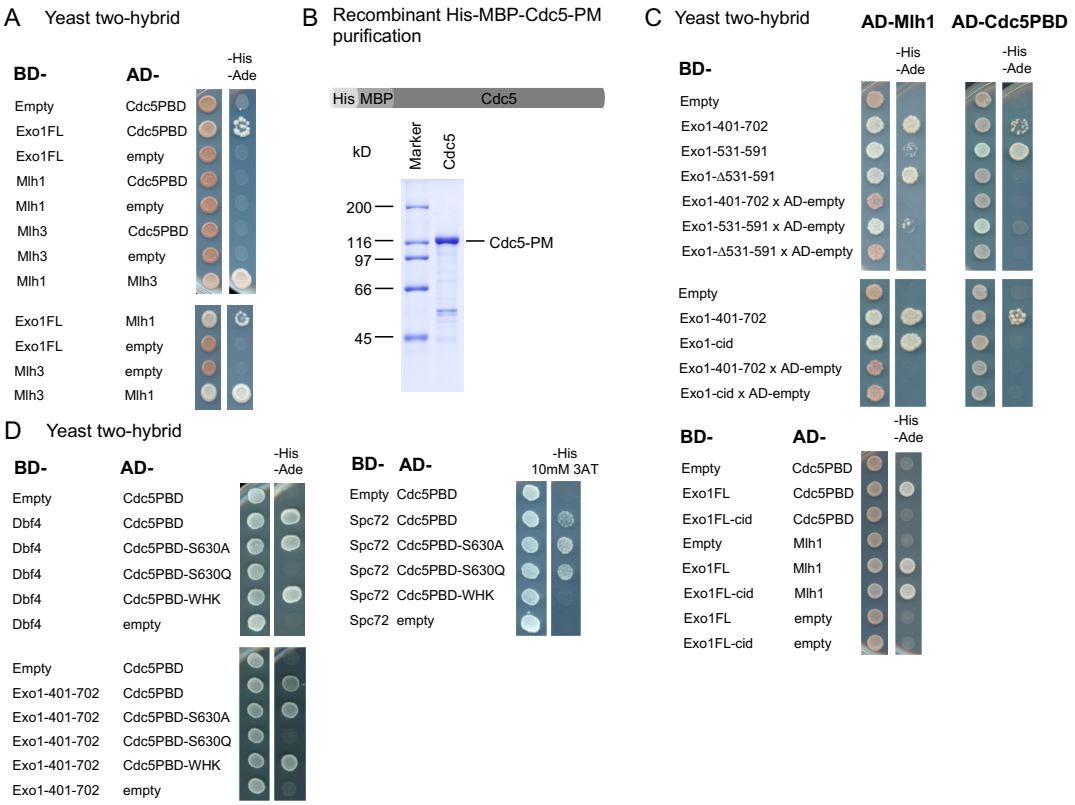

Figure S7: Exo1 and Dbf4 interact through the same motif on the same surface of Cdc5 PBD.

(A) Two-hybrid interactions between MutLg-Exo1 and Cdc5-PBD. The same number of cells of strains expressing the different fusion proteins were plated on minimal media lacking the indicated aminoacids to select for interactions. Growth on -His-Ade medium indicates an interaction. Mlh1-Mlh3 and Exo1-Mlh1 interactions are used as a positive control. FL: Full length.

(B) Purification of recombinant His_MBP-Cdc5-PM (Cdc5 T238D phosphomimetic mutant). MBP, Maltose binding protein tag; His, 10x histidine tag. The 7.5 % SDS-PAGE shows the final fraction (10 µl of Ni-NTA Eluate) of Cdc5-PM purification.

(C) Delineation of the region of Exo1 showing a two-hybrid interaction with Cdc5-PBD or Mlh1. Same as in (A).

(D) Two-hybrid interactions between Exo1 and Cdc5-PBD mutants. Growth on -His-Ade medium indicates an interaction. For Spc72, interactions were assessed on -His+10 mM 3-aminotriazole (3AT), to avoid autoactivation of the BD-Spc72 fusion. Cdc5-PBD mutants interactions with Dbf4 and Spc72 are used as controls (5, 6).

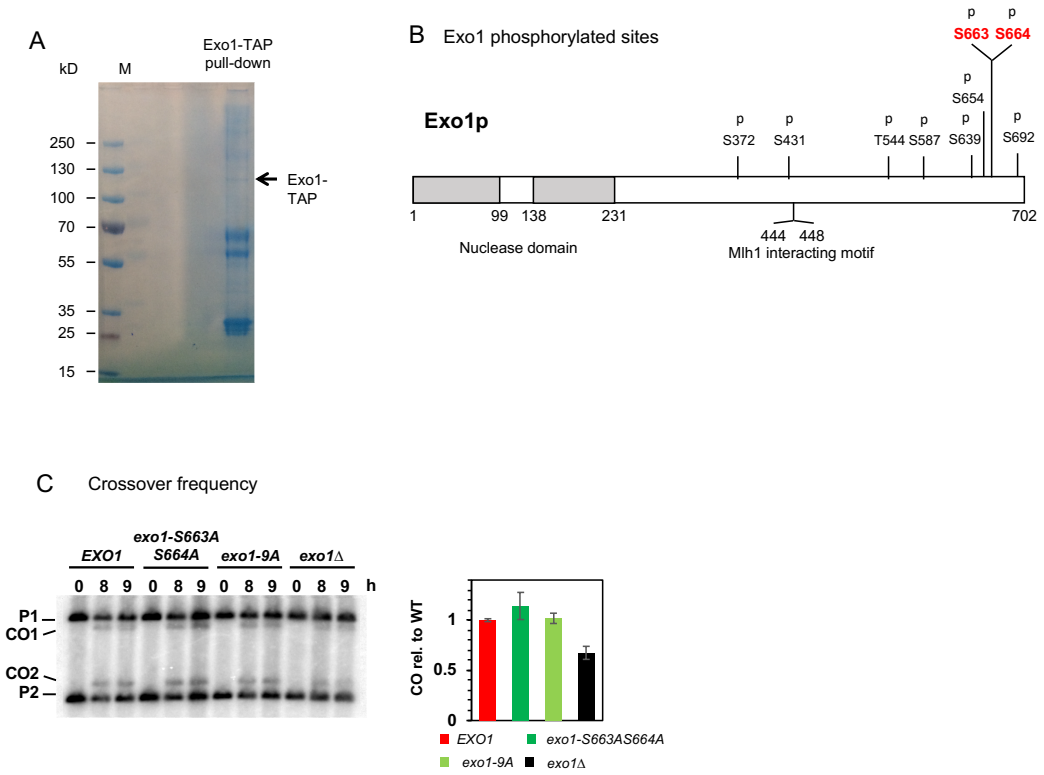

Figure S8: Exo1 phosphorylation sites from cells at the crossover resolution stage of meiosis

(A) Colloidal blue stained gel showing the material pulled-down by Exo1-TAP from *ndt80Δ* cells after induction of Cdc5. The band corresponding to Exo1-TAP is indicated with an arrow.

(B) Phosphorylated Exo1 residues from the experiment shown in (A). S663 and S664 are within a minimal CDK site and a consensus site for Cdc5 binding (S-S/T-P). Each letter "p" indicates a phosphorylated residue.

(C) Crossover frequency at the *HIS4LEU2* hotspot monitored by Southern blot at the indicated times in meiosis. Graph shows quantification at 8 and 9 h ± S.D.

SUPPLEMENTAL MATERIALS AND METHODS

Sporulation conditions and construction of yeast strains

Two different approaches were used for meiosis induction. In the first one, cells were grown in SPS presporulation medium and transferred in sporulation medium as described (7). For highly synchronous copper-inducible meiosis, the procedure was described in (8). Cells were grown in YPD to exponential phase and were inoculated at a starting OD_{600} of 0.05 into reduced glucose YPD (1% yeast extract, 2% peptone, 1% glucose) and grown to an OD_{600} = 11.0- 12.0 for 16- 18 h. Cells were washed, resuspended in sporulation medium (1.0% (w/v) potassium acetate, 0.02% (w/v) raffinose, 0.001% polypropylene glycol) at OD_{600} of 2.5. After 2 h, copper (II) sulfate (50 μM) was added to induce *IME1* expression from the *CUP1* promoter. For strain constructions and spore viability measurements, sporulation was performed on solid sporulation medium for two days.

Yeast strains were obtained by direct transformation or crossing to obtain the desired genotype. Site-directed mutagenesis, internal and C-terminal tag insertions and gene deletions were introduced by PCR. All transformants were validated using PCR to discriminate between correct and incorrect integrations, and sequenced to ensure epitope tag insertion or mutagenesis. For Mlh3 internal tagging, the Myc8, Myc18 or His6-Flag3 (referred to as Flag) tag sequence, flanked on each side by a GGGGSGGGGS linker sequence, was inserted between residues 512 and 515 of Mlh3 (513 and 514 were deleted). For Pms1 internal tagging, the His6-Flag3 tag sequence, flanked on each side by a GGGGSGGGGS linker sequence, was inserted between residues 758 and 761 of Pms1 (759 and 760 were deleted). Cdc5, Exo1 and Msh4 were C-terminally tagged with the TAP tag sequence (9). Exo1 was tagged with 13 copies of the Myc epitope and Msh4 with 3 copies of the HA epitope using a PCR-based strategy (10). For *exo1cid-CDC5-TAP* fusions, the CDC5-TAP construct was fused after the last aminoacid of Exo1-cid at the endogenous *exo1* locus, separated by a GGGGSGGGGS linker. The no fusion control construct contained the *CDC5-TAP* construct replacing the *EXO1* ORF at the endogenous *EXO1* locus. The KanMX-*pCUP1-3HA-IME1* locus was PCR-amplified from 33604 strain (A. Amon lab) and used for direct transformation. The *exo1-D173A* (*exo1-nd*) mutation was introduced by CRISPR-Cas9 mediated cleavage, as described (11).

Flag pull-down and mass spectrometry analysis

2.10^{10} cells were washed two times with ice-cold TNG buffer (50 mM Tris/HCl pH 8; 150 mM NaCl, 10% Glycerol; 1 mM PMSF; 1X Complete Mini EDTA-Free (Roche); 1X PhosSTOP (Roche)) and flash-frozen in liquid nitrogen. Frozen cells were mechanically ground in liquid nitrogen with the 6775 Freezer/Mill cryogenic grinder (SPEX SamplePrep). The resulting powder was resuspended in 25 mL of lysis buffer (50 mM Tris/HCl pH 7.5; 1 mM EDTA; 0.5% NP40; 10% glycerol; 150 mM NaCl; 1X Complete Mini EDTA-Free (Roche); 1X PhosSTOP (Roche), 0 or 210 U/mL benzonase (Sigma)) and incubated 1 h at 4°C with rotation. The lysate was cleared by centrifugation at 8000 g for 10 min and pre-cleared by pre-incubated with 100 µl Mouse IgG−Agarose beads (A0919 Sigma) without antibody for 2 h at 4°C on wheel. The pre-cleared lysate was incubated with 100 µl of washed and buffer equilibrated anti-Flag magnetic beads (Sigma-Aldrich, St. Louis, MO) for 2 h at 4°C. The beads were washed once with lysis buffer and three times with washing buffer (20 mM Tris/HCl pH 7.5; 0.5 mM EDTA; 0.1% tween; 10% glycerol; 150 mM NaCl; 5 mM MgCl2; 0.5 mM PMSF; 1X Complete Mini EDTA-Free (Roche, Switzerland); 1X PhosSTOP (Roche)). Proteins were eluted with 5 bed volume of elution buffer (20 mM Tris/HCl pH 8; 0.5 mM EDTA; 0.1% tween; 10% glycerol; 150 mM NaCl; 5 mM MgCl2; 0.5 mM PMSF; 1X Complete Mini EDTA-Free (Roche); 1X PhosSTOP (Roche); 100 µg/mL Flag peptide) for 2 h at 4°C. Proteins were separated by SDS-PAGE, stained with colloidal blue, and bands covering the entire lane were excised for each sample. In-gel digestion was performed overnight by using trypsin/LysC (Promega, Madison, WI). Peptides extracted from each band were analyzed by nanoLC-MS/MS using an Ultimate 3000 system (Dionex, Thermo Scientific, Waltham, MA) coupled to a TripleTOF™ 6600 mass spectrometer (ABSciex). For identification, data were converted to mgf files, merged with Proteome Discoverer (version 2.2) and searched against the Swissprot fasta database containing *S. cerevisiae* (2019_04, 7905 sequences) using Mascot™ (version 2.5.1) and further analyzed in myProMS v3.6 (12). Data are available via ProteomeXchange with the identifier PXD014180 (13). Only proteins found in four experiments and not in the control IPs were considered candidates.

Co-immunoprecipitation and Western blot analysis

$1.2.10^{9}$ cells were harvested, washed once with PBS, and lyzed in 3 ml lysis buffer

(20 mM HEPES/KOH pH7.5; 150 mM (TAP purification) or 300 mM (anti-FLAG immunoprecipitation) NaCl; 0.5% Triton X-100; 10% Glycerol; 1 mM MgCl2; 2 mM EDTA; 1 mM PMSF; 1X Complete Mini EDTA-Free (Roche); 1X PhosSTOP (Roche); 0 or 125 U/mL benzonase) with glass beads three times for 30 s in a Fastprep instrument (MP Biomedicals, Santa Ana, CA). The lysate was incubated 1 h at 4°C. For TAP-tagged proteins precipitation, 100 µL of PanMouse IgG magnetic beads (Thermo Scientific) were washed 1:1 with lysis buffer, preincubated in 100 µg/ml BSA in lysis buffer for 2 h at 4°C and then washed twice with 1:1 lysis buffer. The lysate was cleared by centrifugation at 13,000 g for 5 min and incubated overnight at 4°C with washed PanMouse IgG magnetic beads. The magnetic beads were washed four times with 1 mL of wash buffer (20 mM HEPES/KOH pH7.5; 150 mM NaCl; 0.5% Triton X-100; 5% Glycerol; 1 mM MgCl2; 2 mM EDTA; 1 mM PMSF; 1X Complete Mini EDTA-Free (Roche); 1X Phos- STOP (Roche)). The beads were resuspended in 30 µL of TEV-C buffer (20 mM Tris/HCl pH 8; 0.5 mM EDTA; 150 mM NaCl; 0.1% NP-40; 5% glycerol; 1 mM MgCl2; 1 mM DTT) with 4 µL TEV protease (1 mg/ml) and incubated for 2 h at 23°C under agitation. The eluate was transferred to a new tube. For anti-FLAG immunoprecipitation, 50 µl of Protein G magnetic beads were used and 10 µg of mouse monoclonal anti-FLAG primary antibody M2 (Sigma) were added before overnight incubation at 4°C with the lysate. Wash buffer contained 300 mM NaCL. After washing, beads were resuspended in 25 µl of 2x SDS protein sample buffer. Beads eluate was heated at 95°C for 10 min and loaded on acrylamide gel (4-12% Bis-Tris gel (Invitrogen)) and run in MOPS SDS Running Buffer (Life Technologies). Proteins were then transferred to PVDF membrane using Trans-Blot® Turbo™ Transfer System (Biorad) at 1 A constant, up to 25 V for 45 min. Proteins were detected using c-Myc mouse monoclonal antibody (9E10, Santa Cruz, 1:500), Flag mouse monoclonal antibody (M2, Sigma, 1:1000), HA.11 mouse monoclonal antibody (16B12, Biolegend, 1/750) or TAP rabbit monoclonal antibody (Invitrogen, 1/2000). Signal was detected using the SuperSignal West Pico or Femto Chemiluminescent Substrate (ThermoFisher). Signal was quantified after image acquisition with Chemidoc system (Biorad).

Mutation analysis

Mutation rates in the presence of tagged *MLH3* alleles were estimated by

measuring the spontaneous reversion rate at the *lys2::InsE-A14* locus in strains derived from the E134 strain (14, 15). Three single colonies from three independent transformants of the same genotype or nine colonies of the parent E134 strain were grown to stationary phase in liquid YPD medium and plated onto YPD or selective medium lacking lysine for revertant count.

Exo1-TAP pull down and phosphopeptides analysis

ndt80Δ cells containing an inducible *CDC5* gene were used (16). After SPS pre-growth and 7 h in sporulation medium, 1 µM □-estradiol was added to induce p*GAL1-CDC5*. 2.10^{10} cells were harvested after 8 h 15 min in sporulation medium and processed as described above for the Flag-affinity pull-down in the presence of 125 U/mL benzonase. 1500 µL of PanMouse IgG magnetic beads (Thermo Scientific) were washed 1:1 with lysis buffer, preincubated in 100 µg/ml BSA in lysis buffer for 2 h at 4°C and then washed twice with 1:1 lysis buffer. The lysate was cleared by centrifugation at 8000 g for 10 min at 4°C and incubated overnight at 4°C with the washed PanMouse IgG magnetic beads. The magnetic beads were washed four times with 8 mL of wash buffer (20 mM HEPES/KOH pH7.5; 150 mM NaCl; 0.5% Triton X-100; 5% Glycerol; 1 mM MgCl2; 2 mM EDTA; 1 mM PMSF; 1X Complete Mini EDTA-Free (Roche)). Beads were then resuspended in 40 µl of Laemmli buffer and heated for 10 min at 75°C. Proteins were separated by SDS-PAGE, stained with colloidal blue, and the band predicted to contain Exo1-TAP was excised and processed. Excised gel slice was washed and proteins were reduced with 10 mM DTT prior to alkylation with 55 mM iodoacetamide. After washing and shrinking of the gel pieces with 100% acetonitrile, in-gel digestion was performed using trypsin/LysC (0.1µg) overnight in 25 mM ammonium bicarbonate at 30°C. Peptide are then extracted using 60/35/5 MeCN/H2O/HCOOH, vacuum concentrated to dryness and reconstituted in loading buffer A (2/98 MeCN/H2O + 0.05% TFA) prior to liquid chromatography-tandem mass spectrometry (LC-MS/MS) analysis. The extracted peptides were chromatographically separated using an RSLCnano system (Ultimate 3000, Thermo Scientific) coupled to a Q Exactive HF-X mass spectrometer (Thermo Scientific). For identification the data were searched against the UniProtKB/Swiss-Prot *S. cerevisiae* database using Sequest with Proteome Discoverer (version 2.2) and SwissProt fasta database containing *S. cerevisiae*

sequences using MascotTM (version 2.5.1). The resulting files were further processed using myProMS (12) v3.6. The maximum false discovery rate (FDR) calculation was set to 1% at the peptide level for the whole study (Percolator or QVALITY algorithm). We validate phosphorylated peptides by combining the phosphoRS informations and by manually inspecting the peak assignment. Data are available via ProteomeXchange with the identifier PXDO14185.

Recombinant proteins and interaction assays

Exo1-Flag purification from Sf9 insect cells was described previously (17). The *CDC5* gene was amplified from *S. cerevisiae* genomic DNA (SK1) with added *Nhe*I and *Xho*I sites, and cloned into the *Nhe*I and *Xho*I sites of a vector backbone modified from pFB-MBP-*MLH3*-his (18) by adding sequence for a 8xHis tag before the MBP gene, to make pFB-His-MBP-*CDC5*. Cdc5 is only active when phosphorylated. We addressed this issue by mutating the conserved threonine 238 (T210 in human PLK) to aspartic acid (T238D) (19, 20). This mutation is known to activate yeast Cdc5 constitutively (21). The Cdc5T238D (Cdc5-PM) protein was expressed and purified in Sf9 cells following the protocol described for Mlh1-Mlh3 (18), except that both the His and the MBP tags are present in the recombinant protein. 1 mg of protein was obtained from 1.4 L *Sf*9 insect cells culture (SI Appendix Fig. S7B). CDK1-cyclin B was purchased from Merck. Lambda phosphatase was purchased from NEB.

To phosphorylate Exo1-Flag, 1 µg of the recombinant Exo1-Flag was incubated in kinase buffer (50 mM Tris-HCl pH 7.5, 5 mM Mg(OAc)2, 0.2 mM EDTA) supplemented with phosphatase inhibitor mixture (0.5 mM Na_3VO_4, 10 mM p-nitrophenyl phosphate). 40 ng of CDK1-cyclin B were added to the reaction. Phosphorylation reaction was started by adding 0.1 mM ATP and incubated for 15 min at 30°C. To dephosphorylate Exo1-Flag, 1 µg of the recombinant Exo1-Flag was incubated in 10X NEBuffer for Protein MetalloPhosphatases (PMP) supplemented with 1 mM $MnCl_2$. 280 U of Lambda phosphatase were added to the reaction. Dephosphorylation was initiated by incubating for 15 min at 30°C. To test for the interaction between His-MBP-Cdc5 and Exo1-Flag treated or not with CDK1 or Lambda phosphatase, 10 µl Protein G magnetic beads (Thermo Scientific) were used to capture 4 µg anti-Flag Monoclonal M2 antibody (Sigma, F3165). Exo1-Flag (1µg) was incubated with the beads in 60 µl binding buffer III (25 mM

Tris-HCl pH 7.5, 3 mM EDTA, 1 mM DTT, 20 mg/ml BSA, 75 mM NaCl) for 60 min with continuous mixing. Next, the beads were washed 3 times with 150 µl wash buffer III (25 mM Tris-HCl pH 7.5, 3 mM EDTA, 1 mM DTT, 120 mM NaCl, 0.05% Triton X-100). 1 µg His-MBP-Cdc5 was then added to the resuspended beads in 60 µl binding buffer III, and incubated for additional 60 min with continuous mixing. Beads were washed 3 times with 150 ul wash buffer III and boiled for 3 min at 95°C in SDS buffer to elute the proteins. The protein complexes were detected by western blot with anti-His antibody (Genscript, A00186) and anti-Flag antibody (Sigma, F3165)

Cloning for two-hybrid analyses

EXO1, DBF4 and *SPC72* fragments and *CDC5-PBD* (residues 340 to 705) were PCR-amplified from SK1 genomic DNA. Site-directed mutations were introduced by fusion of PCR products. PCR products were cloned in plasmids derived from the 2 hybrid vectors pGADT7 (GAL4-activating domain) and pGBKT7 (GAL4-binding domain) creating N terminal fusions and transformed in yeast haploid strains Y187 and AH109 (Clontech), respectively. Interactions were scored, after mating and diploid selection on dropout medium without leucine or tryptophan, as growth on dropout medium without leucine, tryptophan, adenine or histidine or on dropout medium without leucin, tryptophan or histidine and with 10 mM 3-Amino-1,2,4-triazole (3-AT).

Chromatin immunoprecipitation, real-time quantitative PCR and ChIP-seq

Chromatin immunoprecipitation was performed as described (11), with the following modifications: lysis was performed in Lysis buffer plus 1 mM PMSF, 50 µg/mL Aprotinin and 1X Complete Mini EDTA-Free (Roche), using 0.5 mm zirconium/silica beads (Biospec Products, Bartlesville, OK). We used 1.6 µg of c-Myc monoclonal antibody and 50 µL PanMouse IgG magnetic beads or 1 µl of anti-Flag antibody and 30 µl Protein G magnetic beads (Thermo Scientific). For Cdc5-TAP ChIP, the lysate was directly applied on 50 µL PanMouse IgG magnetic beads. Before use magnetic beads were blocked with 5 µg/µl BSA for 4 h at 4°C.

Quantitative PCR was performed from the immunoprecipitated DNA or the whole cell extract using a 7900HT Fast Real-Time PCR System and SYBR Green PCR master mix (Applied Biosystems, Thermo Scientific) as described (11). Results were expressed as % of DNA in the total input present in the immunoprecipitated

sample and normalized first by the negative control site in the middle of *NFT1*, a 3.5 kb long gene that shows no DSB nor axis-attachment site, and then by the 0 h time point of the meiotic time-course or the 2 h time-point for copper-induced synchronous meiosis. Primers for qPCR have been described (11). For ChIP-seq experiments, 1. 10^9 cells were processed as described before (1).

Spo11 oligonucleotide mapping

Spo11-Flag oligonucleotides were purified and processed for sequencing library preparation as previously described (22). Briefly, cells were harvested from a 600 ml sporulating culture (VBD2016) after synchronizing in meiosis thanks to the p*CUP1-IME1* system at the 5 h time-point to approximate time of peak Spo11-oligo levels. The experiment was made on two biological replicates. Sequencing (Illumina HiSeq 2500, 2 x 50 bp paired-end reads) was performed in the MSKCC Integrated Genomics Operation. Clipping of library adapters and alignment of reads to S288C using genome version sacCer2 were performed by the Bioinformatics Core Facility at MSKCC using a custom pipeline as described (23, 24). The list of hotspots of each replicate is in SI Appendix, Dataset S2. The two duplicates were highly similar (SI Appendix, Figure S4A) and were pooled for further analyses.

Illumina sequencing of ChIP DNA and read normalization

Purified DNA was sequenced using an Illumina HiSeq 2500 instrument and following the Illumina TruSeq procedure, generating paired-end 50 bp reads. Mer3-Flag ChIP-seq was performed in two independent replicates from cells (strain VBD1421) at the 4 h time-point synchronized using the SPS preculture method (7). The negative control was from an untagged anti-Flag ChIP-seq sample (strain VBD1311). Mlh3-Myc8 ChIP-seq was performed once at two different time-points (t = 5 h and t = 5.5 h) on meiotic cells (VBD1837 or VBD2026 for the *exo1-nd* strain) synchronized with the copper-inducible system. The negative control was Mlh3-Myc8 ChIP-seq in a DSB-deficient *spo11Δ* strain (VBD1841) at the same respective time-points, to reveal only DSB-associated Mlh3 binding sites. Reads were aligned to the sacCer2 version (SGD June 2008) of the *S. cerevisiae* S288C genome, using Bowtie, allowing for 2 mismatches. Reads that matched more than once in the genome or matching to mitochondrial or ribosomal DNA were eliminated from further analysis. Paired-end extended reads were

normalized to the negative control, bigwig files generated and then the negative control was subtracted to generate normalized and background-subtracted bigwig files using a custom script as described (1).

Bioinformatic analyses

Sequencing data were analyzed using https://usegalaxy.org/ and custom bash and R scripts. ChIP-seq peak calling was performed on the experiment and negative control Bam alignment files using the MACS2 program at https://usegalaxy.org/, with parameters available upon request. Signal smoothing was performed on the normalized and background-subtracted bigwig files using a custom script employing fast Fourier transform convolution with a sliding window of the size indicated in legends of Fig. 2, and SI Appendix, Figs. S4 and S5. The script is available upon request.

For computing the ChIP-seq signal per DSB represented for different proteins on Figures 2D, 2F and SI Appendix, Fig. S5, the ChIP-seq signal was multiplied by a factor before subtracting the control signal, to avoid obtaining negative values and negative ratios after dividing by the Spo11 oligo signal, since the ChIP-seq signal is very low for some proteins close to centromeres and/or telomeres. This was done for further statistical analyses and does not affect the conclusions. The following factors were used: Mer3: 1.2; Zip4: 1.3; Mlh3 _5 h 30: 1.2; Mlh3 _5 h: 1.15; Mlh3 *exo1-nd*: 1.2. To compare pericentromeric or subtelomeric regions to interstitial regions of similar DSB (Spo11 oligo signal) frequency, interstitial regions were first filtered based on the appropriate Spo11 signal using an opportune percentile range of the same signal in the region of interest (25-75 percentile for Spo11 and 25-60 percentile for pCUP1-Spo11). Then, interstitial regions were randomly selected (number of regions in each group = number of regions in each control) with substitutions and its median was calculated. This step was repeated 10000 times and these data were used as control. For defining interstitial hotspots in early or late replicating regions, we used the replication index data at the 3.5 h meiotic time-point from (25), and selected among the strongest 2000 hotspots from (2) those located further than 20 kb away from a telomere or a centromere, and that had a log2 replication index lower than -0.07 (early regions, 306 hotspots) and those with a replication index higher than 0.07 (late regions, 351 hotspots).

To generate the graph Fig. S4C representing the lengths of resection tracts, we used the data from (4) from wild-type cells at t= 4 h, and deduced the distribution of the tracts from the determination of resection end-points.

SUPPLEMENTAL REFERENCES

1. A. De Muyt *et al.*, A meiotic XPF-ERCC1-like complex recognizes joint molecule recombination intermediates to promote crossover formation. *Genes & development* **32**, 283-296 (2018).
2. X. Zhu, S. Keeney, High-Resolution Global Analysis of the Influences of Bas1 and Ino4 Transcription Factors on Meiotic DNA Break Distributions in Saccharomyces cerevisiae. *Genetics* **201**, 525-542 (2015).
3. X. Sun *et al.*, Transcription dynamically patterns the meiotic chromosome-axis interface. *Elife* **4** (2015).
4. E. P. Mimitou, S. Yamada, S. Keeney, A global view of meiotic double-strand break end resection. *Science* **355**, 40-45 (2017).
5. A. W. Almawi *et al.*, Distinct surfaces on Cdc5/PLK Polo-box domain orchestrate combinatorial substrate recognition during cell division. *Sci Rep* **10**, 3379 (2020).
6. Y. C. Chen, M. Weinreich, Dbf4 regulates the Cdc5 Polo-like kinase through a distinct non-canonical binding interaction. *J Biol Chem* **285**, 41244-41254 (2010).
7. H. Murakami, V. Borde, A. Nicolas, S. Keeney, Gel electrophoresis assays for analyzing DNA double-strand breaks in Saccharomyces cerevisiae at various spatial resolutions. *Methods in molecular biology* **557**, 117-142 (2009).
8. M. Chia, F. J. van Werven, Temporal Expression of a Master Regulator Drives Synchronous Sporulation in Budding Yeast. *G3 (Bethesda)* 10.1534/g3.116.034983 (2016).
9. O. Puig *et al.*, The tandem affinity purification (TAP) method: a general procedure of protein complex purification. *Methods* **24**, 218-229 (2001).
10. M. S. Longtine *et al.*, Additional modules for versatile and economical PCR-based gene deletion and modification in Saccharomyces cerevisiae. *Yeast* **14**, 953-961 (1998).
11. Y. Duroc *et al.*, Concerted action of the MutLbeta heterodimer and Mer3 helicase regulates the global extent of meiotic gene conversion. *Elife* **6**, e21900 (2017).
12. P. Poullet, S. Carpentier, E. Barillot, myProMS, a web server for management and validation of mass spectrometry-based proteomic data. *Proteomics* **7**, 2553-2556 (2007).
13. J. A. Vizcaino *et al.*, 2016 update of the PRIDE database and its related tools. *Nucleic Acids Res* **44**, D447-456 (2016).
14. P. V. Shcherbakova, T. A. Kunkel, Mutator phenotypes conferred by MLH1 overexpression and by heterozygosity for mlh1 mutations. *Mol Cell Biol* **19**, 3177-3183 (1999).
15. H. T. Tran, J. D. Keen, M. Kricker, M. A. Resnick, D. A. Gordenin, Hypermutability of homonucleotide runs in mismatch repair and DNA

polymerase proofreading yeast mutants. *Mol Cell Biol* **17**, 2859-2865 (1997).
16. A. Sourirajan, M. Lichten, Polo-like kinase Cdc5 drives exit from pachytene during budding yeast meiosis. *Genes & development* **22**, 2627-2632 (2008).
17. E. Cannavo, P. Cejka, S. C. Kowalczykowski, Relationship of DNA degradation by Saccharomyces cerevisiae exonuclease 1 and its stimulation by RPA and Mre11-Rad50-Xrs2 to DNA end resection. *Proc Natl Acad Sci U S A* **110**, E1661-1668 (2013).
18. L. Ranjha, R. Anand, P. Cejka, The Saccharomyces cerevisiae Mlh1-Mlh3 heterodimer is an endonuclease that preferentially binds to Holliday junctions. *J Biol Chem* **289**, 5674-5686 (2014).
19. M. Geymonat, A. Spanos, P. A. Walker, L. H. Johnston, S. G. Sedgwick, In vitro regulation of budding yeast Bfa1/Bub2 GAP activity by Cdc5. *J Biol Chem* **278**, 14591-14594 (2003).
20. K. S. Lee, R. L. Erikson, Plk is a functional homolog of Saccharomyces cerevisiae Cdc5, and elevated Plk activity induces multiple septation structures. *Mol Cell Biol* **17**, 3408-3417 (1997).
21. E. M. Mortensen, W. Haas, M. Gygi, S. P. Gygi, D. R. Kellogg, Cdc28-dependent regulation of the Cdc5/Polo kinase. *Curr Biol* **15**, 2033-2037 (2005).
22. I. Lam, N. Mohibullah, S. Keeney, Sequencing Spo11 Oligonucleotides for Mapping Meiotic DNA Double-Strand Breaks in Yeast. *Methods Mol Biol* **1471**, 51-98 (2017).
23. J. Pan *et al.*, A hierarchical combination of factors shapes the genome-wide topography of yeast meiotic recombination initiation. *Cell* **144**, 719-731 (2011).
24. D. Thacker, N. Mohibullah, X. Zhu, S. Keeney, Homologue engagement controls meiotic DNA break number and distribution. *Nature* **510**, 241-246 (2014).
25. H. Murakami, S. Keeney, Temporospatial coordination of meiotic DNA replication and recombination via DDK recruitment to replisomes. *Cell* **158**, 861-873 (2014).